

Small-Angle Photoproduction of Positive Pions from Hydrogen*

J. H. MALMBERG† AND C. S. ROBINSON

Physics Research Laboratory, University of Illinois, Urbana, Illinois

(Received September 9, 1957)

The angular distribution of π^+ mesons produced in hydrogen by 225-Mev photons has been measured in the small-angle region. The mesons were produced in a liquid hydrogen target placed in the x-ray beam of the 300-Mev betatron. A focusing magnet was used to select mesons of the desired momentum. The large electron pair background was avoided by use of a very short x-ray pulse and a counter system which operated only after the pulse, counting the decays of μ^+ mesons. Points have been obtained at center-of-mass angles of 10, 15, 20, 30, 45, 60, and 90 degrees. The observed angular distribution cannot be fitted by a quadratic in $\cos\theta^*$, but is well fitted by the cross section calculated from the field theory of Chew, Goldberger, Low, and Nambu.

I. INTRODUCTION

THE photoproduction of π^+ mesons from hydrogen has been the subject of numerous experiments,¹⁻⁹ and the angular distribution of the mesons between 45° and 135° is reasonably well known. This angular distribution is well represented by a quadratic function of $\cos\theta^*$, where θ^* is the center-of-mass meson angle, as predicted by the phenomenological theory of Brueckner and Watson¹⁰ and of Feld.¹¹ The meson field theory developed by Chew and others¹²⁻¹⁵ also describes this angular distribution and the excitation function for the reaction rather successfully. In this theory, the interaction between the photon and the meson current was evaluated so as to include only "almost real" mesons, i.e., those not contributing to the matrix element between single physical nucleon states.¹⁵ The result is a term in the angular distribution with a denominator $(1-\beta\cos\theta^*)^2$, where β is the meson velocity, and with an amplitude depending on the renormalized interaction constant and substantially

smaller than if the entire meson current had been included. This term, the direct interaction term, has an important effect on the predicted cross section mainly at small angles, and at photon energies above about 200 Mev. Measurements at small angles in the energy range above 200 Mev therefore represent the best possibility of verifying if the above term is present in the cross section and has the predicted magnitude. The present experiment was designed to investigate these questions. We have measured the meson angular distribution in the range 10° to 90° at a photon energy of 225 Mev.

II. EXPERIMENTAL ARRANGEMENT

The major difficulty encountered in an attempt to detect charged photomesons at small angles is the very large background of pair electrons. In the present experiment, this background is avoided by using a very short x-ray pulse and a counter system which is turned on only after the pulse to count the decays of the μ^+ mesons.

The experimental arrangement is shown in Fig. 1. A doubly-collimated 280-Mev x-ray beam falls on a liquid hydrogen target located 4.2 meters from the internal target of the University of Illinois betatron. The liquid target is a vertical cylinder of 2½ inch diameter with Mylar walls. The x-ray beam is 0.93 inch in diameter at the hydrogen target. π^+ mesons are focused by the analyzing magnet into a telescope of three liquid scintillators, *A*, *B*, and *C*. The momentum bin is determined by a brass collimator *F* immediately in front of the telescope. The extreme trajectories possible in the magnet are determined by the two aluminum blocks *S* which fill the magnet gap on either side of the region used. These blocks serve as aperture stops, and define the range of angles accepted by the magnet. Since both the energy and angle of the meson are known, the energy of the incident photon is determined. The hydrogen target and the counter telescope are both rigidly attached to the analyzing magnet, which may be rotated about a vertical axis through the target. The region from the secondary collimator to the counter telescope is evacuated to reduce scattering and

* Supported in part by the National Science Foundation and by the joint program of the Office of Naval Research and the U. S. Atomic Energy Commission.

† Now at John Jay Hopkins Laboratory for Pure and Applied Science, General Atomic Division of General Dynamics Corporation, San Diego, California.

¹ J. Steinberger and A. S. Bishop, *Phys. Rev.* **86**, 171 (1952).

² White, Jacobsen, and Schulz, *Phys. Rev.* **88**, 836 (1952).

³ Jarmie, Repp, and White, *Phys. Rev.* **91**, 1023L (1953).

⁴ G. Bernardini and E. L. Goldwasser, *Phys. Rev.* **94**, 729 (1954).

⁵ Jenkins, Luckey, Palfrey, and Wilson, *Phys. Rev.* **95**, 179 (1954).

⁶ J. E. Leiss and C. S. Robinson, *Phys. Rev.* **95**, 638(A) (1954); J. E. Leiss, Ph.D. thesis, University of Illinois, 1954 (unpublished).

⁷ Walker, Teasdale, Peterson, and Vette, *Phys. Rev.* **99**, 210 (1955).

⁸ Tollestrup, Keck, and Worlock, *Phys. Rev.* **99**, 220 (1955).

⁹ Beneventano, Bernardini, Carlson-Lee, Stoppini, and Tau, *Nuovo cimento* **4**, 323 (1956).

¹⁰ K. A. Brueckner and K. M. Watson, *Phys. Rev.* **86**, 923 (1952).

¹¹ B. T. Feld, *Phys. Rev.* **89**, 330 (1953).

¹² G. F. Chew, *Phys. Rev.* **95**, 1669 (1954).

¹³ G. F. Chew and F. E. Low, *Phys. Rev.* **101**, 1570 (1956); G. F. Chew and F. E. Low, *Phys. Rev.* **101**, 1579 (1956).

¹⁴ Chew, Goldberger, Low, and Nambu, *Phys. Rev.* **106**, 1345 (1957).

¹⁵ G. F. Chew, "Theory of Pion Scattering and Photoproduction," in *Encyclopedia of Physics* (Springer-Verlag, Berlin, to be published), second edition, Vol. 43 See especially Sec. V.

background. A beam-clearing magnet is placed at the exit of the secondary collimator to remove charged particle contamination from the x-ray beam after it has entered the vacuum system.

The pion beam passes through a copper absorber *D* so chosen that the pions will stop approximately in the center of counter *B*. The short-range decay muons stop still close to the center of counter *B*. About two microseconds after the x-ray pulse, the photomultipliers are turned on and coincidences between *A* and *B* and between *B* and *C* are counted.

The short x-ray pulse is obtained by use of a "shaker" circuit which puts a 30-microsecond half-sine-wave current pulse through windings arranged to weaken the guide field on the target side of the machine and strengthen it on the other side. To a first approximation this slides the whole orbit towards the target, which is at the *outside* of the accelerating tube. In addition, the amplitude of the radial oscillations is rapidly increased. The x-ray pulse so produced looks approximately Gaussian and has a full width at one half maximum of 0.6 microsecond. A small fraction of the electrons which pass through the target have a sufficiently small scattering angle and energy loss so that their subsequent orbits are completely contained in the accelerator tube; these electrons will eventually pass through the target again. A rough calculation indicates that such multiple transits through the target should produce a tail on the pulse with a relative intensity of the order of 10^{-3} and a time constant of the order of a microsecond. Such a tail is observed. If the target were placed at the *inside* of the stable orbit, as is done in many synchrotrons, no orbits of this type would be possible, and there should be no tail on the x-ray pulse.

The betatron yield is measured by a thick-walled copper ionization chamber intercepting the entire collimated x-ray beam. The chamber is continuously monitored by a vibrating reed electrometer of 0.1% accuracy. Since the chamber is not sealed, the readings must be reduced to NTP conditions. This correction contributed less than 0.1% error to the final results. The betatron energy during the present experiment was controlled to better than 1%. Since the experiment is not very sensitive to betatron energy, errors due to uncertainties in this energy are negligible.

The liquid hydrogen target has been described in detail by Whalin and Reitz.¹⁶ The target vacuum is isolated from the magnet vacuum by Mylar windows. In addition to the 0.0025-inch Mylar walls of the hydrogen container there are 0.001 inch of aluminum foil and 0.010 inch of Mylar in the beam. The latter foils are sufficiently far from the hydrogen container so that their contribution to the empty-target background is appreciably reduced.

The analyzing magnet used in the present experiment

¹⁶ E. A. Whalin and R. A. Reitz, *Rev. Sci. Instr.* **26**, 59 (1955).

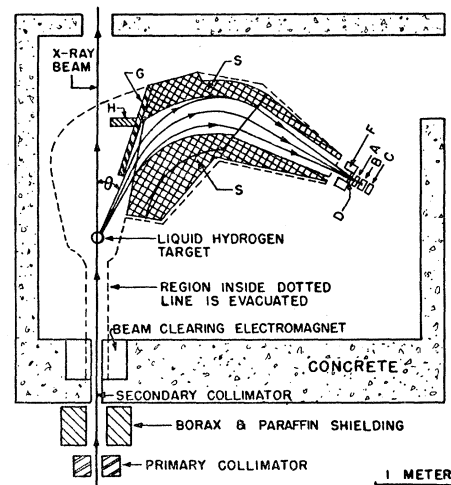


FIG. 1. Plan view of the experimental arrangement, roughly to scale. The focusing magnet has a uniform gradient perpendicular to the entrance edge. The aluminum blocks *S* define the range of angles accepted by the magnet. The lead blocks *G* and *H* stop most of the very low-energy pair electrons which are swept out of the forward direction by the fringing field. *D* is a copper absorber which is chosen so that the mesons stop near the center of counter *B*. The magnet return yoke has been omitted. The neutron shielding around the counters, which is not shown, consists of 16 in. of borax-paraffin mixture.

was designed, built, and calibrated by Miller.¹⁷ The magnetic field has a uniform gradient parallel to the median plane, and perpendicular to the entrance edge of the magnet, such that the exit gap height is about one-half of the entrance gap height. The momentum of the magnet was calibrated to 1% in terms of both the field at a certain point and the current. Both these quantities were measured to 0.1% frequently during the experiment. They always agreed to within 0.2%. The magnet horizontal angle bin is 4.9° . The solid angle is 0.0126 steradian $\pm 2.4\%$ and has been shown by direct measurement to be momentum-independent to 1% over the range of momentum used in this experiment. The fractional momentum bin of the magnet as used in this experiment is approximately 0.025.

The magnet angle is read to 0.2° . The "0°" angle is determined to 0.2° by measuring the pair electron counting rate for a succession of angles near the forward direction, and finding the center of the angle bin so traced out. The magnet vacuum is always kept an order of magnitude better than necessary to make its effect negligible.

The lead shield *G* in Fig. 1 stops most of the very low-energy pair electrons which are swept out of the forward direction by the magnet fringing field. Without the shield, these electrons would strike the pole faces or the aperture stops *S* and give rise to a large background of low-energy bremsstrahlung directed toward the counters. The counts produced by these x-rays are not

¹⁷ R. C. Miller and C. S. Robinson, *Ann. Phys.* **2**, 129 (1957); R. C. Miller, Ph.D. thesis, University of Illinois, 1956 (unpublished).

easily removed by use of absorbers in the counter telescope. Absorption curves indicate that the counts are produced by x-rays of a few Mev energy. Even though these x-rays are produced and detected with a small efficiency, and even though only those arriving after the main x-ray pulse are recorded, the pair production cross section is so large that the corrective shield *G* is essential.

The most effective way to prevent spurious counts due to these x-rays is to arrange the shielding so that the pair electrons are not traveling toward the counter telescope when they strike the shielding. Their bremsstrahlung is then directed away from the telescope. At large angles, this is accomplished by use of the lead brick *H*. Since this brick is outside the shield *G* it has no effect on the magnet aperture.

III. COUNTING EQUIPMENT

The geometry of the counter telescope is shown in Fig. 2. The scintillation fluid is contained in and viewed through Lucite light pipes. The absorbers are put in the telescope to prevent knock-on protons and electrons from neutron-capture gamma rays from counting as coincidences. They are not sufficiently thick to prevent counts resulting from double knock-on or double Compton scattering processes. A typical π - μ - e decay is sketched.

When the magnet is at a small angle, hundreds of particles pass through the scintillators during the main part of the x-ray pulse. Two microseconds later, the scintillators and photomultipliers must have recovered sufficiently from this blast to be useful detectors. In fast solid scintillators, about 5% of the light comes out with a decay time of a few microseconds.¹⁸ In liquid scintillators this slow component is absent. Therefore liquid scintillators were chosen for the present experiment. The solution used consists of three grams of *p*-terphenyl per liter of phenylcyclohexane.

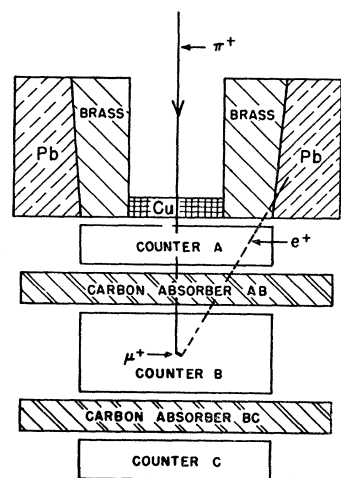


FIG. 2. Plan view of the counter telescope. A typical π - μ - e decay is sketched. The energy bin of the detecting system is determined by the brass collimator. The copper absorber is chosen so that the incoming π^+ mesons will stop approximately in the center of counter *B*. Counters *A* and *C* are 1 inch thick and counter *B* is 2 inches thick. All three counters are $4\frac{1}{8}$ inches in diameter. The carbon absorbers *AB* and *BC* are each 3.0 g/cm^2 .

Since afterpulsing in the photomultipliers lasts for several microseconds, the photomultipliers must be off during the x-ray pulse. This was accomplished by biasing dynodes 2 and 4 about three hundred volts negative with respect to their normal operating voltages and pulsing them up to their normal voltages to turn on the tube.¹⁹ With this pulsing method the noise is approximately equal to the dc value. Tests showed that the gain of the tube is the same as the dc value to within 5%. This was demonstrated by flashing a one millimicrosecond light pulse²⁰ on the tube under pulsed and dc conditions.

The phototube gate pulse-height stability is better than 1%. During the rise of the gate pulse, the phototube gain changes from 10% to 95% in 0.03 microsecond. The gate length was 6.2 ± 0.2 microseconds. The error in meson counting rate due to changes in the gate length is hence limited to 0.2%.

To avoid errors resulting from instabilities in the shape of the x-ray pulse, the gate pulse was triggered by a circuit²¹ which selects the time when a fixed fraction *f* of the mesons remains. This selection was done by differentiating the integrated x-ray intensity with a 2.2-microsecond time constant, and determining when the resulting quantity has dropped to a fraction *f* of the total undifferentiated value. The accuracy of this determination depends only on the resistance and capacitor values in the circuit, which can be made very stable.

As a test of the timing circuit, the meson counting rates with the normal 0.6-microsecond x-ray pulse and with a 1.2-microsecond x-ray pulse were compared and found equal within the 3% counting statistics. This change in pulse length is much greater than any instability encountered during the experiment. In addition, the data at 30° c.m. were taken partly with one value of *f* and partly with another; the observed counting rates have the same ratio, within the 5% counting statistics, as that computed from the accurately measured components in the timing circuit.

The photomultiplier output pulses are limited in voltage and time duration and then fed to a coincidence circuit with a resolution of 8×10^{-9} second. Each of the coincidence outputs *AB* and *BC* is amplified, passed through a crystal diode to remove small pulses, amplified, and passed through a pulse height discriminator into a trigger circuit. The outputs of the trigger circuits are combined to form the triple coincidence *ABC* and the anticoincidences *AB-C* and *BC-A*. These events and also *AB* and *BC* are recorded on scalers. Since the *AB* and *BC* counting rates can be obtained by adding the *ABC* rate to the *AB-C* and *BC-A* rates respectively, we have a redundancy check on much of the electronics and on the recording of the data.

¹⁹ RCA 6199 photomultipliers were used. This method of pulsing was suggested by Dr. Raphael Littauer.

²⁰ J. H. Malmberg, Rev. Sci. Instr. 28, 1027 (1957).

²¹ J. H. Malmberg (to be published).

¹⁸ F. B. Harrison, Nucleonics 12, No. 3, 24 (1954).

IV. TESTS OF THE EQUIPMENT

The counters were extensively tested with a beam of high-energy electrons and it was shown that they were working properly. The arrangement used to count mesons is necessarily much less favorable. The decay electrons are emitted in all directions by muons which have stopped in counter *B*, and corner-clipping effects, in which electrons traverse only a short length of scintillator, are very important. Some of the decay electrons will be counted mainly as the result of Čerenkov radiation emitted as they traverse the Lucite light pipes. Further, the mesons stop with a rather large spatial distribution due to the dispersion of the magnet, multiple scattering, and ionization straggling. The result is that the efficiency for counting mesons depends appreciably on the gain of the counter system. A typical curve of meson counting rate *vs* photomultiplier voltage is given in Fig. 3. The slope of the plateau is about 25% per one hundred volts. Hence it is neces-

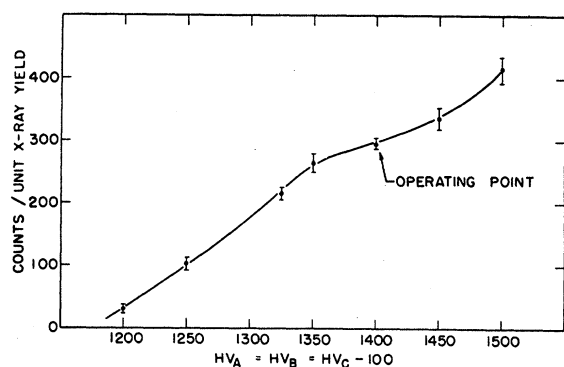


Fig. 3. Meson counting rate *vs* photomultiplier high voltage. The counting rate is the sum of the rates for the *AB-C* and *BC-A* channels. The voltages were changed simultaneously on all three photomultipliers. The data were taken at a laboratory angle of 74° .

sary to show that the equipment is sufficiently stable to prevent drifts in the electronics from affecting the meson counting rate.

The effect on the meson counting rate of changes in the various circuits was determined and these changes were kept sufficiently small to contribute less than $\frac{1}{2}\%$ change in counting rate during the experiment. This stability was achieved in part by frequent calibrations with a mercury switch pulser. The photomultipliers were magnetically shielded and the effect of the magnet fringing field on them was shown to be completely negligible.

We prove that we are counting mesons by showing that the particles counted have the correct range, sign of charge, decay time, and dynamic threshold. At 74° in the laboratory system the counting rate from a carbon target was measured for two meson energies as a function of the thickness of copper absorber preceding the telescope. A typical result is given in Fig. 4. The solid curve represents a crude calculation of the expected

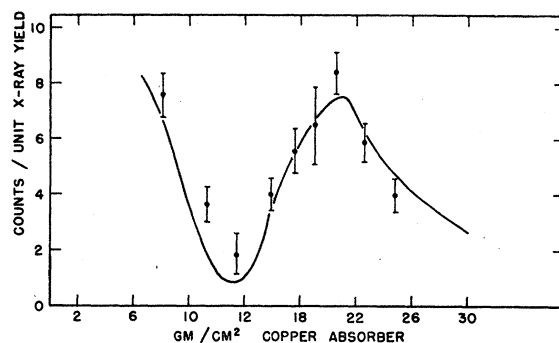


Fig. 4. Range curve for mesons in the counter telescope. The *BC* counting rate is plotted against the thickness of copper in front of the telescope. The magnet is set to focus 82.4-Mev π^+ mesons into the telescope. The data were taken at 74° in the laboratory system. The solid curve represents a crude calculation of the expected counting rate. The minimum near 12 gm/cm² occurs because most mesons are then stopping in the carbon absorber between *B* and *C*, and their decay electrons cannot make *BC* coincidences. The maximum near 20 gm/cm² occurs because most mesons then stop in counter *B*, and many of their decay electrons traverse *B* and *C*.

counting rate, using reasonable assumptions about counter sensitivity and spatial distribution of stopped mesons, and considering solid angle effects and nuclear absorption. The shape of the curve is explained as follows. For about 20 gm/cm², the mesons stop near the center of counter *B*. If some absorber is removed, the mesons will stop in carbon absorber *BC*, and their decay electrons cannot produce *BC* counts. If more absorber is removed, mesons will stop in counter *C*, and can again produce *BC* counts. If more than 20 gm/cm² is used, mesons stop nearer *A*, and the solid angle for detection of decays by *BC* decreases. The measured counting rates agree with the calculation about as well as can be expected considering the crudeness of the calculation. The qualitative features of the data leave no doubt that we are counting mesons.

Further evidence on the range of the particles counted is that the triple coincidence rates from hydrogen at all angles were negligible, while the tests with fast electrons showed that 90% counted as triples. The low triples rate proves that no appreciable percentage of our counting rates is caused by fast electrons.

The counting rate as a function of delay time is shown in Fig. 5. The data were taken at 7.6° in the laboratory system. The observed decay agrees with the muon lifetime within the counting statistics. It should be noted that a decay curve does not by itself demonstrate that the counts arise from muons, since the tail on the x-ray pulse, the afterpulsing in the photomultipliers, and the slow component of light from the scintillators all exhibit roughly similar lifetimes. Under certain conditions the neutron background will also have a similar decay.

The counting rate as a function of betatron energy is shown in Fig. 6 for 7.6° in the laboratory system. The magnet is set for mesons produced by 225-Mev photons.

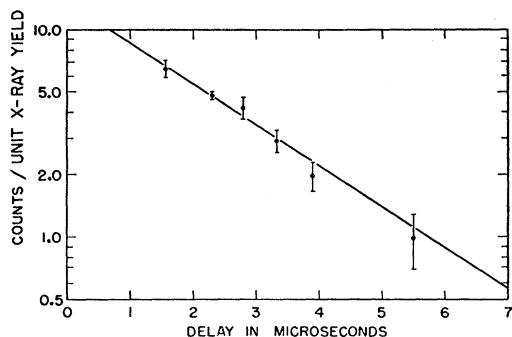


FIG. 5. Counting rate *vs* delay time after the x-ray pulse. The data were taken at 7.6° in the laboratory system. The straight line represents the known μ^+ lifetime of 2.22 microseconds and has been normalized to the data.

The solid curve was computed from the bremsstrahlung spectrum and the energy dependence of the monitor sensitivity, and has been normalized to the point at 280 Mev.

The most convincing evidence that we are counting only pions is that the counting rate drops by about a factor of ten at all angles when the hydrogen target is emptied or when the magnetic field is reversed or reduced to zero. Since positive and negative electrons are made in about equal numbers by the x-ray beam, any counting rate due to electrons would be roughly symmetric with respect to magnet polarity. The only charged particles other than mesons and electrons that can be produced in hydrogen by x-rays of this energy are protons. No proton focused by the magnet could penetrate the counter telescope sufficiently to be detected. It is known that muon production from hydrogen is small compared to pion production. Moreover, muons of the correct momentum will have a considerably greater range. The observed background of 6 to 10% decays with a time constant of about 100 microseconds. We conclude that we are counting pions and that the background consists primarily of neutrons.

V. EXPERIMENTAL RESULTS

Data for the angular distribution were taken with two different settings of the gate timing circuit. In order to keep the counters completely free of electron-induced effects at small angles, a longer delay time before turning on the counters was used below 30° . The longer delay corresponds to a smaller value of f , and gives a proportionately smaller counting rate. Below 30° , f was 0.321; above 30° , f was 0.450; at 30° about half of the data were taken with each setting. For the angles at which the smaller delay was used, the background was essentially the same for the two delay settings. This is to be expected since the background consists primarily of neutrons and decays quite slowly. For each angle the background was subtracted from the total counting rate, and the resulting net counting rate was divided by f to obtain the number of mesons per unit x-ray yield.

Two sets of background data were taken: one set with the magnetic field reversed and the target filled with hydrogen; the other with the magnetic field normal and the target evacuated. The empty-target, normal-field counting rates are consistently about 10% higher than the full-target, reversed-field counting rates. If we were counting an appreciable number of electrons ($\approx 1\%$ of the meson rate from hydrogen), the reverse would be true, since the full hydrogen target is a much better pair producer than the empty target, and since the Compton process contributes to negative electron production so that more negative than positive electrons are produced. A further indication that we are not counting electrons is that the background does not rise at forward angles whereas the electron production is sharply peaked in the forward direction. In fact, the background rises as we move toward 90° . This occurs because at the large angles the counters are closer to the betatron, which is a source of photoneutrons, and because not as much of the shielding is between the counters and the betatron at large angles.

The 10% difference between the two sets of background data is accounted for by π^+ meson production in the walls of the target. (π^- mesons are not detected by the counters.) In order to utilize both sets of background data, the reversed-field data have been corrected as follows. The expected meson counting rate from the empty target was computed from the observed full-target, normal-field counting rate, a knowledge of the various foils that are in the beam, and an approximate knowledge of the relative cross sections for photomeson production of the materials involved. This correction (1% of the rate from hydrogen) was added to the full-target, reversed-field data. The combined background data from both sets are shown in Fig. 7. From the geometry of the apparatus we expect that the background, which we have shown to be almost entirely neutrons, will be a slowly varying function of angle. A cubic curve, shown in Fig. 7, provides a statistically

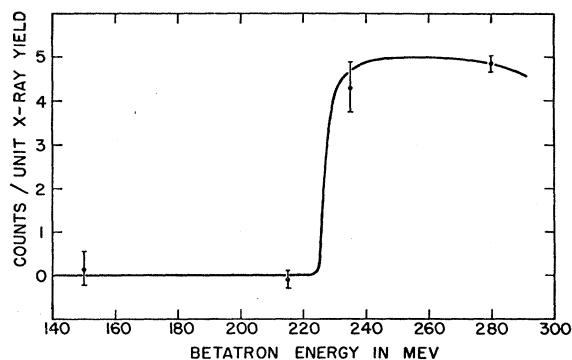


FIG. 6. Counting rate *vs* betatron energy at 7.6° in the laboratory system. The magnet is set for mesons produced by 225-Mev photons. The empty-target background has been subtracted. The solid curve is computed from a knowledge of the bremsstrahlung spectrum and the energy dependence of the monitor sensitivity, and has been normalized to the point at 280 Mev.

good fit to the background points, confirming that the background has the expected behavior. Values read from this curve were used in obtaining the net counting rates from hydrogen. The statistics used for the background values read from the curve are the calculated standard deviations for the curve at those points, and are in general smaller than the statistics on the individual data points. It makes no significant difference in the results whether the original background points or the values from the curve are used. The background was 6 to 10% of the total counting rate.

In order to obtain relative cross sections from the observed counting rates, it is necessary to know how the efficiency of the system for detecting mesons varies with meson energy. There are several factors entering into the detection efficiency which vary with energy. Among these is the solid angle of the scintillators for detecting decay electrons, which can be calculated only roughly. In order to determine accurately the energy variation of the detection efficiency, the equipment was calibrated by counting mesons of three energies from hydrogen at 90° c.m. where the cross section is known from previous experiments. For a given meson energy in the laboratory system the cross section at any angle θ is then obtained from the equation

$$\left(\frac{d\sigma}{d\Omega^*}\right)_\theta = \frac{R_\theta}{R_{90}} \frac{N_{90}}{N_\theta} \frac{(d\Omega^*/d\Omega)_{90}}{(d\Omega^*/d\Omega)_\theta} \left(\frac{d\sigma}{d\Omega^*}\right)_{90}, \quad (1)$$

where $d\sigma/d\Omega^*$ is the differential cross section, R is the number of mesons per unit x-ray yield, N is the number of photons per unit x-ray yield which have an energy such as to produce mesons in the energy bin of the detecting system, and $d\Omega^*/d\Omega$ is the solid angle transformation.

The values of R_{90} at intermediate energies are obtained by interpolation. N is obtained from tables

TABLE I. Relative cross sections for photoproduction of positive pions from hydrogen at 225 Mev. The counting rates are included in the table to show that the essential features of the angular dependence of the cross section at small angles appear also in the raw data.

θ^*	Counting rates ^a	$d\sigma/d\Omega^*$ ^b
10°	2.15±0.04	0.539±0.011
15°	2.04±0.06	0.515±0.015
20°	2.03±0.06	0.515±0.016
30°	2.09±0.05	0.543±0.013
45°	2.38±0.05	0.638±0.015
60°	2.72±0.07	0.760±0.021
90°	3.37±0.09	1.000±0.027

^a No. of mesons per joule. These numbers are weighted averages of the individual runs, corrected for temperature and pressure, with background subtracted, and divided by the delay factor f .

^b Normalized to unity at 90°. Our absolute values of the cross section agree with those from other experiments within the accuracy of estimating the detection efficiency of the counter system (about 30%). Since five large-angle experiments at or near this energy (refs. 5-9), when compared using the theory of Chew *et al.* for interpolation, agree in absolute cross section with a total spread of only 18%, it is not considered worthwhile to give absolute values here.

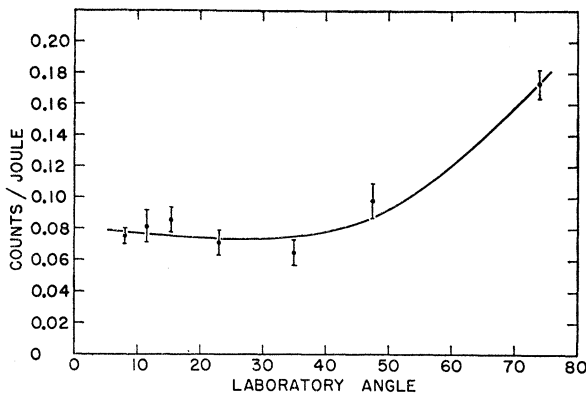


FIG. 7. Background counting rate vs laboratory angle. The points are weighted averages of the full-target reversed-field data with a correction added to represent π^+ meson production in the target walls, and the empty-target normal-field data. The curve is the least-squares cubic for the points. Values and standard deviations computed from the curve were used in obtaining the cross sections.

prepared by Leiss²² using the zero-angle spectrum of Schiff,²³ and from dynamics tables prepared by Malmberg and Koester²⁴ recomputed for the most recent pion mass (139.7 Mev). $d\Omega^*/d\Omega$ is also obtained from the dynamics tables. The energy dependence of $(d\sigma/d\Omega^*)_{90}$ is obtained from the paper of Beneventano *et al.*⁹ As is pointed out in that paper, there is substantial agreement among the various laboratories on the energy dependence of the 90° cross section even when there is disagreement as to the absolute value.

The counting rates R are corrected for the fact that the projected width of the irradiated portion of the target changes as the magnet is rotated. In order to make this correction, the sensitivity of the detecting system as a function of source position was determined by counting mesons at 74° from carbon cylinders placed at various positions along the x-ray beam. The effect of the apparent change in target shape was then obtained by numerical integrations of the sensitivity over the target volume. The correction amounts to 1.6% in the worst case and is made to an accuracy of about 10%. The relative cross sections are tabulated in Table I. A summary of the counting rates is also given in Table I to show that the essential features of the angular dependence of the cross section at small angles appear also in the raw data.

VI. EXPERIMENTAL ERRORS

The reproducibility of the data is demonstrated in two ways. First, each point is the average of a large number of runs. A careful statistical analysis of the

²² J. E. Leiss, "Bremsstrahlung Spectra," privately circulated tables, University of Illinois, Physics Research Laboratory, 1952 (unpublished).

²³ L. I. Schiff, Phys. Rev. **83**, 252 (1951).

²⁴ J. H. Malmberg and L. J. Koester, Jr., "Tables of Nuclear Reaction Kinematics at Relativistic Energies," privately circulated tables, University of Illinois, Physics Research Laboratory, 1953 (unpublished).

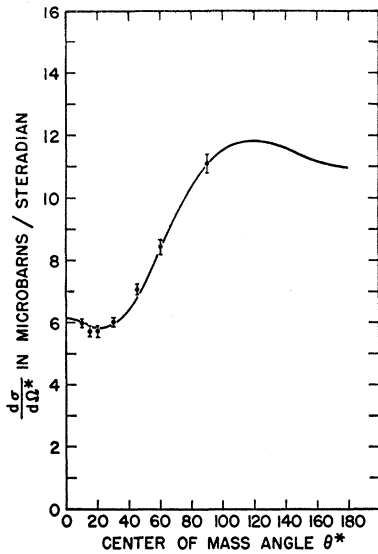


FIG. 8. Comparison of the observed cross sections with the theory of Chew, Goldberger, Low, and Nambu. Photon energy is 225 Mev. The data have been normalized to the theory.

individual runs for the whole experiment shows excellent internal consistency. Second, the 10° point was measured 3 times, near the beginning, middle, and end of the experiment. The three measurements agree very well. The reproducibility of the data, together with the stability tests mentioned earlier, shows that no appreciable drifts occurred in the counting equipment.

A systematic error would arise if the axis of rotation of the magnet were not exactly through the center of the hydrogen target, since in this case the number of protons in the beam would be a function of angle. The position of the hydrogen target is uncertain to about 3 millimeters. A 3-millimeter displacement would produce a systematic relative error of about $0.01 \sin^2(\theta + \theta_1)$ in the cross section, where θ is the laboratory angle of the magnet and θ_1 is the angle between the magnet and the displacement of the target.

Two other possible sources of systematic error are statistical errors in the observed counting rate at 90° , and uncertainty in the energy dependence of the 90° cross section. These errors may cause a systematic distortion of the cross section of as much as 5% between 90° and 10° . However, since the distortion is a function of energy only, and since the pion energy changes very slowly at forward angles, the effect of these errors will be important only when comparing forward to backward angles and will not exceed 1% for the interesting region of angles, namely from 45° forward.

VII. COMPARISON WITH THEORY

The differential cross section for positive photopion production from hydrogen has been computed by Goldwasser²⁵ from equations developed by Chew, Goldberger, Low, and Nambu¹⁴ using the general dispersion relations. Figure 8 compares our experimental

²⁵ E. L. Goldwasser (private communication).

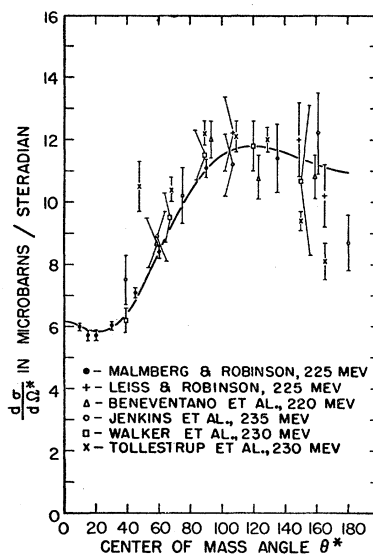


FIG. 9. Comparison of our data with other experiments. The solid curve is the same theoretical curve shown in Fig. 8. The data from each experiment have been normalized to the theory. No correction has been made for the fact that the experiments were not all done at exactly the same energy. The corrections required to convert the normalized cross sections to 225 Mev would not exceed 3% in the worst case, except for the Cornell and Cal. Tech. points at 39° which would be raised by 8% and 5%, respectively.

results with this calculation. The data have been normalized to the theory. The agreement between theory and experiment is excellent. The standard deviations shown in Fig. 8 for the experimental points are those due to counting statistics only. As previously pointed out, there may also be small systematic distortions in the observed angular distribution.

In order to see if the theory of Brueckner and Watson¹⁰ and Feld¹¹ could explain the observed angular distribution, an attempt was made to fit our data with a quadratic in $\cos\theta^*$. The best-fitting curve of this type represents a statistically improbable fit, and furthermore has an unreasonably high value at back angles. If the requirement is added that the curve have a reasonable value at 180° (i.e., not higher than at 90°), the best-fitting quadratic represents the data so poorly as to be completely unacceptable. This fit cannot be materially improved by inclusion of any distortion possible within the systematic errors of the experiment. Attempts to fit a quadratic to the combined data of all experiments at or near this energy were equally unsuccessful. We conclude that the theory as formulated by Chew *et al.* is necessary to explain the observed cross section.

In Fig. 9 our data are shown together with the results of all other available experiments at or near this energy. A curve is also shown of the theory of Chew *et al.* To avoid the effects of apparent differences of as much as 18% between experiments in the absolute cross section scale, the data from each experiment have been normalized to the theory. No correction has been made for the fact that the experiments were not all done at exactly the same energy. The correction required to convert the normalized cross sections to 225 Mev would not exceed 3% in the worst case, except for the Cornell and Cal. Tech. points at 39° which would be raised by 8% and 5%, respectively. The agreement of

our data with other experiments is satisfactory in the region of overlap. The disagreement among experiments at angles beyond 140° appears to exceed what might be expected from the standard deviations of the points.

Cross sections at small angles have been measured at other energies by experimenters at the General Electric Research Laboratory,²⁶ at M. I. T.,²⁷ and at the University of California.²⁸ Of these, final results are available at this time only for the California 260-Mev measurements, which indicate an angular distribution similar to that found in the present experiment.

VIII. CONCLUSIONS

We conclude that the angular distribution of positive photopions from hydrogen at 225-Mev photon energy is

²⁶ R. D. Miller and R. Littauer, *Bull. Am. Phys. Soc. Ser. II*, **2**, 6 (1957).

²⁷ B. Richter and L. S. Osborne (private communication to E. L. Goldwasser).

²⁸ Knapp, Imhof, Kenney, and Perez-Mendez, *Phys. Rev.* **107**, 323 (1957).

very satisfactorily described by the theory of Chew *et al.*, and cannot be fitted satisfactorily with a quadratic in $\cos\theta^*$. This constitutes direct evidence that the interaction of the photon with the meson cloud exists and has approximately the magnitude calculated by Chew *et al.*

IX. ACKNOWLEDGMENTS

The authors are grateful to Dr. R. C. Miller who actively collaborated in several phases of this work and to Dr. J. E. Leiss who made a number of the early tests of the short-pulse method. We are indebted to Professor G. Bernardini for helpful discussions. We wish to thank Mr. T. A. King and others of the betatron crew, who went out of their way to be helpful. Valuable contributions to the experiment were also made by Mrs. Dorothy Carlson-Lee and Lloyd Hendricks, Edward Eby, Donald Nigg, and Paul Baum.

Observation and Analysis of K^- Interactions*

J. HORNBOSTEL AND G. T. ZORN
Brookhaven National Laboratory, Upton, New York
(Received September 13, 1957)

In nuclear emulsions, 289 K^- mesons were observed. The mass and lifetime of K^- mesons is the same as that of K^+ mesons. The K^- mean free path in nuclear emulsion is geometric. Charge-exchange scattering and inelastic K^- -nucleus scattering are rare. Positive hyperons are emitted in 8% of K^- capture stars, negative hyperons in about 9%, hyperfragments in 5%. It is estimated that a Λ^0 is trapped without production of a visible hyperfragment in an additional 8%. A K^- is captured by one nucleon with formation of a Σ hyperon and a pion in about 0.77 of the cases, with creation of a Λ^0 and a pion in approximately 0.18 of the events. Capture by two nucleons occurs in roughly 0.05 of the cases. From a comparison of production and emission frequencies of Σ hyperons it is concluded that an attractive nuclear potential for Σ hyperons must be less than 20 Mev. Limits for the mean free paths for ordinary scattering, for charge-exchange scattering, and for absorption of Σ hyperons in nuclear matter are given. The trapping of Λ^0 hyperons in nuclei is discussed.

1. INTRODUCTION

IN continuing earlier studies¹ of K^- events observed in nuclear emulsions, 289 K^- mesons were found, most of them in stacks exposed at the Cosmotron. Analysis of this much enlarged sample (which includes the events of the previous study) made it possible to confirm or revise some of the earlier conclusions by basing them on statistically more reliable data, and to arrive at additional results relating to the behavior of hyperons in nuclear matter.

The presentation is divided into two essentially independent parts. The first deals with K^- interactions

in flight (Sec. 3) and with decays (Sec. 4). In the second, experimental data relating to K^- captures at rest are presented (Sec. 5) and analyzed (Secs. 6 and 7). In this analysis, use is made of experimentally determined relative frequencies of the three basic capture reactions of K^- mesons:

$$K^- + N \rightarrow \Sigma + \pi, \quad (\text{Ia})$$

$$K^- + N \rightarrow \Lambda^0 + \pi, \quad (\text{Ib})$$

$$K^- + 2N \rightarrow Y + N', \quad (\text{II})$$

where N and N' are nucleons and Y may be either a Σ hyperon (reaction IIa) or a Λ^0 (reaction IIb). Reactions (Ia) and (Ib) are referred to as mesonic, reaction (II) as nonmesonic captures. By comparing the reaction frequencies with the frequencies of observed charged Σ hyperons (corrected for inefficiency of de-

* Research carried out under the auspices of the U. S. Atomic Energy Commission.

¹ J. Hornbostel and E. O. Salant, *Phys. Rev.* **102**, 502 (1956); hereinafter referred to as HS I.